ARTICLES

Proteomic analysis of active multiple sclerosis lesions reveals therapeutic targets

May H. Han[1]*, Sun-Il Hwang[3]*, Dolly B. Roy[4]*, Deborah H. Lundgren[3], Jordan V. Price[1], Shalina S. Ousman[1], Guy Haskin Fernald[5], Bruce Gerlitz[6], William H. Robinson[2], Sergio E. Baranzini[5], Brian W. Grinnell[6], Cedric S. Raine[7], Raymond A. Sobel[8], David K. Han[3] & Lawrence Steinman[1]

Understanding the neuropathology of multiple sclerosis (MS) is essential for improved therapies. Therefore, identification of targets specific to pathological types of MS may have therapeutic benefits. Here we identify, by laser-capture microdissection and proteomics, proteins unique to three major types of MS lesions: acute plaque, chronic active plaque and chronic plaque. Comparative proteomic profiles identified tissue factor and protein C inhibitor within chronic active plaque samples, suggesting dysregulation of molecules associated with coagulation. *In vivo* administration of hirudin or recombinant activated protein C reduced disease severity in experimental autoimmune encephalomyelitis and suppressed Th1 and Th17 cytokines in astrocytes and immune cells. Administration of mutant forms of recombinant activated protein C showed that both its anticoagulant and its signalling functions were essential for optimal amelioration of experimental autoimmune encephalomyelitis. A proteomic approach illuminated potential therapeutic targets selective for specific pathological stages of MS and implicated participation of the coagulation cascade.

Multiple sclerosis (MS) is an inflammatory and degenerative disease of the central nervous system (CNS) with diverse clinical presentations and heterogeneous histopathological features. Understanding the neuropathology of MS is essential to develop improved therapies. MS lesions or 'plaques' in the CNS white matter have distinct histological and immunocytological characteristics depending on disease activity[1–3]. This heterogeneity implies that there are discrete molecular events at different pathogenic stages of MS[1,4,5]. Therefore, identification of targets specific to pathological types of MS lesions may have therapeutic benefits during different stages of disease.

In recent years, a 'systems biology' approach using large-scale analysis of proteins and gene transcripts has illuminated new aspects of pathogenesis for complex disease networks including malignancies, neurodegenerative disorders and infections[6–8]. Similarly, large-scale transcriptional profiling of MS lesions has identified involvement of novel molecules and pathways such as osteopontin and Notch/Jagged signalling, respectively[9,10]. However, transcriptomic analysis fails to provide a comprehensive understanding of effector molecules involved in MS pathogenesis because of the susceptibility of messenger RNA to degradation and the discrepancy between mRNA and protein expression levels. Transcriptomic analysis also overlooks signalling molecules from serum, hormones and neurotransmitters. Therefore, a focused proteomic analysis of well-characterized human MS brain lesions, enriched by laser-capture microdissection (LCM) and analysed by sensitive tools such as mass spectrometry, will provide functional insights into the pathogenesis of MS.

Here we classified MS brain lesions into distinct histological types: acute plaque, chronic active plaque (CAP) and chronic plaque. We then isolated the lesions by LCM and performed saturated sequencing by mass spectrometry. We selected two candidate proteins, tissue factor and protein C inhibitor (PCI), by an analysis using a computer-guided system. We then validated their potential therapeutic roles in experimental autoimmune encephalomyelitis (EAE). We also studied the cellular and molecular mechanism of how activated protein C (aPC), an intrinsic inhibitor of PCI, ameliorates EAE. These findings emphasize how lesion-specific proteomic profiling of diseased tissue from patients with MS can identify potential therapeutic targets. In addition, we reveal the extensive interface between the coagulation system and brain inflammation.

Results

Histological characterization of MS lesions. Brain autopsy samples from patients with different clinical subtypes of MS (Table 1) were evaluated by staining with haematoxylin and eosin (H&E), Luxol fast blue (LFB) and immunohistochemistry. Lesions with florid parenchymal and perivascular inflammatory cell infiltration, abundant astroglial hypertrophy, myelin fragmentation, oedema and ongoing demyelination with indistinct margins were classified as acute plaque (Fig. 1a–c and Supplementary Fig. 1a–c)[11]. CAP lesions had chronic demyelination, sharply defined margins and recent areas of inflammatory demyelination at the edges (Fig. 1d–f and Supplementary Fig. 1d–h). Chronic plaque lesions had areas of demyelination with well-demarcated borders and abundant astrogliosis, but few or no inflammatory cells (Fig. 1g–i and Supplementary Fig. 1i). Age-matched control brain samples were analysed similarly and were devoid of CNS abnormalities.

Proteomic profiling of MS lesions. We compared the different histological stages of MS lesions by proteomics analysis to determine their global protein expression profiles. LCM enabled selective isolation of MS lesions from the adjacent white matter from the same tissue blocks evaluated for histological characterization. Samples

[1]Department of Neurology and Neurological Sciences, [2]Division of Immunology and Rheumatology, Stanford University School of Medicine, Stanford, California 94305, USA. [3]Department of Cell Biology, Center for Vascular Biology, University of Connecticut Health Center, Farmington, Connecticut 06030, USA. [4]Northridge Neurological Center, Northridge, California 91325, USA. [5]Department of Neurology, University of California at San Francisco School of Medicine, California 94143, USA. [6]Biotechnology Discovery Research, Lilly Research Laboratories, Lilly Corporate Center, Indianapolis, Indiana 46285, USA. [7]Department of Pathology, Albert Einstein College of Medicine, Bronx, New York 10461, USA. [8]Department of Pathology (Neuropathology), Stanford, California 94305, USA.
*These authors contributed equally to this work.

Table 1 | Characteristics of the MS patients and controls in the study

	Age/gender	Type of MS	Disease duration	Prior treatment	Lesion type	Cause of death	Autopsy interval
MS1	42/F	Acute	2 weeks	None	AP	Respiratory failure	12 h
MS2	54/F	Acute	2½ months	Corticosteroids	AP	Respiratory failure	12 h
MS3	31/F	Chronic	11 years	Corticosteroids	CAP	Respiratory failure	1.5 h
MS4	27/F	Progressive	10 years	Corticosteroids	CAP	Broncho-pneumonia	4 h
MS5	47/M	Secondary progressive	20 years	Corticosteroids	CP	Respiratory failure	24 h
MS6	46/M	Chronic progressive	15 years	Lioresal; compazine	CP	Cardiac arrest	4 h
Control 1	23/F	Fallopian tube cancer	N/A	N/A		Respiratory failure	12 h
Control 2	52/F	Ovarian cancer	N/A	N/A		Respiratory failure	15.5 h

Two separate samples of brain lesions were obtained from MS1 and MS2, and three separate samples were obtained from MS3 to MS6 and normal controls. None of the patients with MS were treated with disease-modifying agents. Full CNS autopsies were performed on all cases. AP, acute plaque; CP, chronic plaque.

isolated by LCM were separately analysed by nanoliquid chromatography and tandem mass spectrometry (Fig. 2a). To ascertain reliable protein identification, we used the criteria of stringent mass tolerance and eliminated false-positive proteins by searching against a forward and reverse human protein database[12]. Furthermore, to enhance maximal protein detection coverage, MS samples were analysed repeatedly by mass spectrometric analysis (four to seven times) until a saturation point was reached (Supplementary Fig. 2). Analysis of control, acute plaque, CAP and chronic plaque samples yielded 2,574 proteins with high confidence. Among these, 2,302 proteins were related to MS samples (three types of lesion combined), and 1,492 proteins belonged to control samples (see Supplementary Table 1 for a complete listing). For individual MS lesion types we identified 1,082, 1,728 and 1,514 proteins for acute plaque, CAP and chronic plaque samples, respectively (Table 2). To our knowledge, this is the largest and the most comprehensive proteome of MS brain lesions characterized so far (Supplementary Tables 1 and 3).

CAP expresses coagulation proteins. After mass spectrometric protein identification, we used INTERSECT software to determine proteins specific to each MS lesion type. There were 158, 416 and 236 proteins unique to acute plaque, CAP and chronic plaque[13] (Supplementary Fig. 3 and Supplementary Table 2). We then applied PROTEOME-3D software to assign biological functions and subcellular localization to these proteins[14]. The analysis revealed that proteins of unknown function made up more than half of the unique proteins identified in all three MS lesion types (Supplementary Fig. 4). Of the proteins with known function, structural proteins, adhesion molecules, cell surface receptors and components of channels were among the most numerous (6% or greater). They were followed by proteins involved in the cell cycle, in synaptic transmission, in cellular signalling and in the components of the machinery for transcription and translation (2–6%). Least numerous were proteins with functions associated with molecular chaperones and cellular metabolism (less than 2%). Interestingly, the analysis revealed five proteins involved in coagulation: tissue factor, PCI, thrombospondin, fibronectin and vitronectin (Fig. 2b, c). These coagulation proteins were unique to CAP samples.

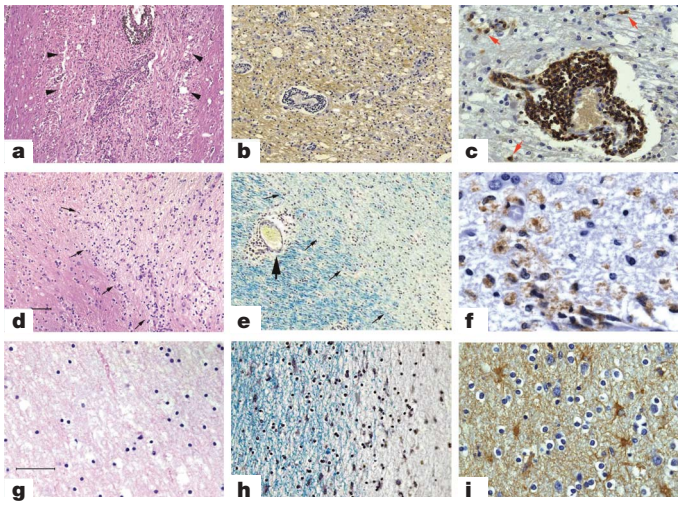

Figure 1 | Histopathology of MS brain lesions. Staining: **a**, **d**, **g**, H&E; **e**, **h**, LFB; **b**, **c**, **f**, **i**, immunohistochemistry. **a**–**c**, Acute plaque. **a**, Marked inflammation, vacuolation (arrowheads) and oedema. **b**, Patchy demyelination (normal myelin, brown), anti-$PLP_{200–219}$. **c**, Perivenous and parenchymal (arrows) inflammatory cells; anti-CD45. **d**–**f**, CAP. **d**, **e**, Well-demarcated edge (arrows), recent inflammation (**e**) (large arrow). **f**, Macrophages within CAP; anti-CD68. **g**–**i**, Chronic plaque. **g**, Hypocellular fibrotic lesion. **h**, Well-demarcated edge. **i**, Astrogliosis, anti-GFAP. Scale bars: **d**, 50 μm (also applies to **a**, **b**, **e**); **g**, 50 μm (also applies to **c**, **h**) and 25 μm **f**, **i**.

Thrombin inhibition attenuates EAE. Tissue factor, a coagulation factor, is expressed in monocytes and astrocytes during inflammation[15,16]. It promotes pro-inflammatory thrombin signalling through the protease activated receptor (PAR) family of proteins[17]. PCI is a serum protein that accumulates in the CAP lesions probably secondary to the disruption of the blood–brain barrier during neuroinflammation. PCI inhibits aPC. aPC also signals through PAR-1 and endothelial protein C receptor (EPCR)[18]. Despite sharing a common signalling pathway with procoagulant tissue factor, aPC is an anticoagulant with cytoprotective properties. The combined presence of tissue factor and PCI suggests pro-inflammatory thrombin formation and suppression of protein C pathway in CAP lesions.

To test the role of thrombin signalling during neuroinflammation, SJL/J mice that had been immunized with myelin proteolipid protein ($PLP_{139–151}$) peptide were treated daily with either intravenous injection of the thrombin inhibitor hirudin (see Methods Summary), or with PBS, at the peak of clinical disease. Mice treated with hirudin showed dramatic improvement in disease severity (Fig. 3a). This was accompanied by decreased immune cell proliferation (Fig. 3b) and suppression of cytokines interleukin (IL)-6, tumour-necrosis factor (TNF) and IL-17 (Fig. 3d, e). There were no differences in the production of IL-4, IL-10, IL-12 and interferon-γ (IFN-γ) cytokines between the vehicle-treated and the hirudin-treated groups (not shown). Hirudin had no effect on relapse rates or disease course (not shown). The brains and spinal cords of mice treated with hirudin showed fewer inflammatory foci (Fig. 3c and Supplementary Fig. 5a, b). Amelioration of EAE by hirudin treatment was observed only up to day 35, probably secondary to development of auto-antibodies against hirudin (see Discussion)[19].

aPC administration ameliorates EAE. aPC has anti-inflammatory and anti-apoptotic functions, and its therapeutic benefits have previously been observed in meningococcemia and in systemic inflammatory response syndrome[15,20–22]. The presence of PCI in CAP samples and evidence of low serum levels of protein C in patients with MS suggest suppression of the protein C pathway during MS[23]. To determine the effects of aPC during neuroinflammation, we induced EAE in 7- to 8-week-old SJL/J mice and treated them with either recombinant murine aPC ($0.2\,mg\,kg^{-1}$) or vehicle (PBS) beginning at the peak of disease. During the course of EAE, mice treated with aPC showed significant amelioration of disease severity (Fig. 4a). Treatment had no effect on relapse rates, nor did it alter the disease course (not shown). This effect was accompanied by decreased immune cell proliferation in splenocytes and lymph-node cells (Fig. 4b) and inhibition of Th1 and Th17 cytokines in

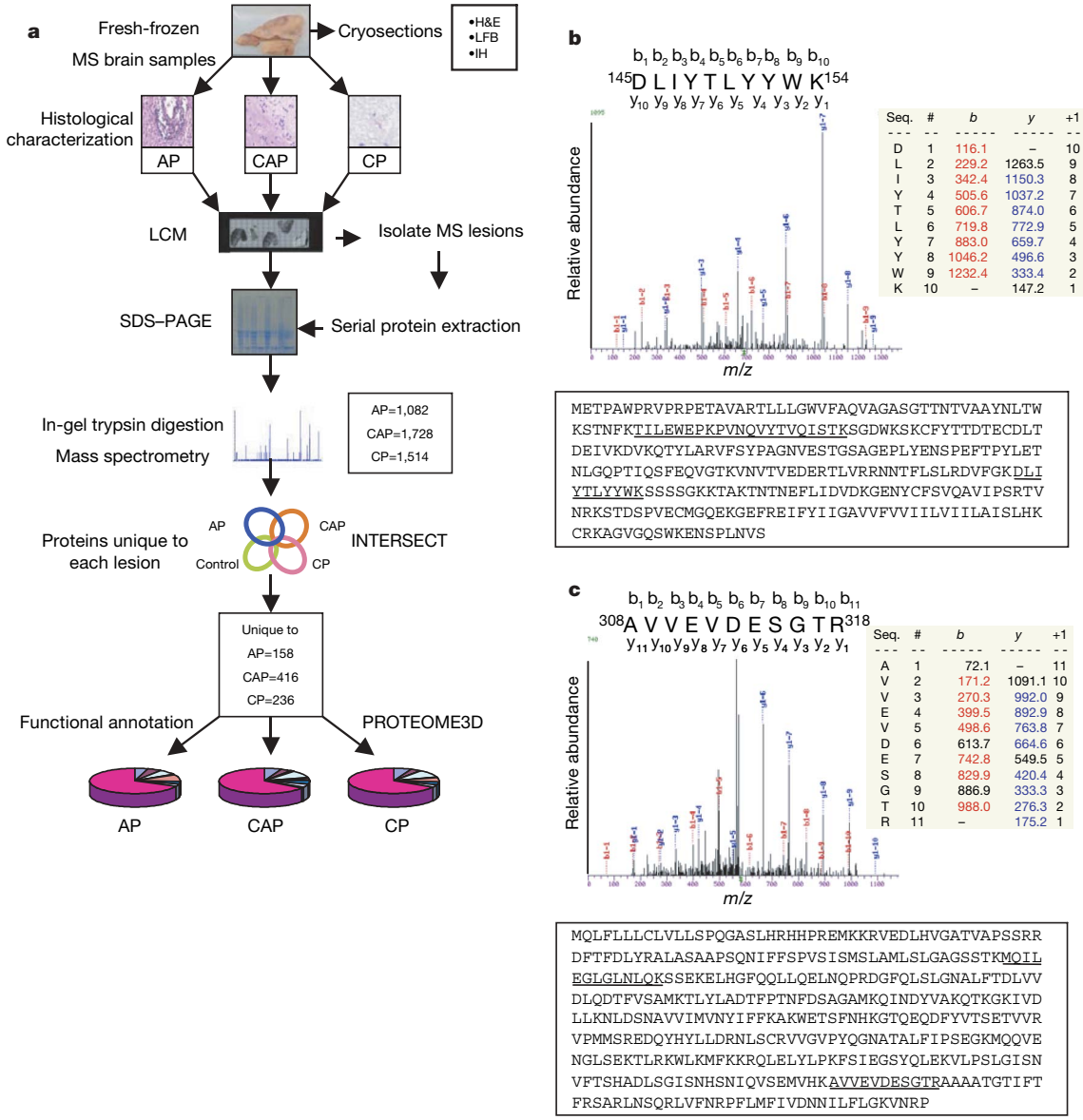

Figure 2 | Proteomic analysis of MS lesions. **a**, Schematic procedure of the proteomic analysis of MS lesions. **b**, Representative tandem mass spectra of peptide(s) identified from (**b**) tissue factor or (**c**) PCI from CAP samples. Sequences of identified peptides are shown above the mass spectra and underlined in the protein sequence; b_n or y_n denote the ion generated by cleavage of the peptide bond after the *n*th amino acid from the amino terminus or the carboxy terminus; identified b and y ions and values of *m*/*z* (mass/charge) for ions are indicated in the table.

aPC-treated mice (Fig. 4c, d). Additionally, fewer inflammatory foci were observed in the CNS tissue of EAE mice treated with aPC (Fig. 4e and Supplementary Fig. 5c, d).

Molecular mechanism of aPC during EAE. aPC functions both as an anticoagulant and a signalling molecule[18]. Structure–function studies have identified the domain of aPC required for its anticoagulant function as distinct from its signalling function[24]. To determine whether the amelioration of EAE by aPC treatment is mediated through anti-coagulant or signalling functions, we induced EAE in SJL/J mice and treated them with two recombinant aPC mutants, aPC-L8W and aPC-K193E[25]. One mutant, aPC-L8W, retains anti-coagulant properties but lacks PAR-1 signalling because of the defective interaction with its receptor EPCR at L8[26]. The other mutant, aPC-K193E, mainly participates in PAR-1 signalling and lacks anti-coagulant activities[18]. The clinical status of the mice treated with aPC mutants was compared with those treated with either vehicle (PBS) or aPC wild type (WT). Mice treated with aPC-L8W and aPC-K193 showed significant amelioration early in the disease course (days 20–25), whereas mice treated with aPC-WT showed improvement in the latter part of disease course (days 25–30) (Fig. 5a–c). These data suggest that both activities of aPC may be required for maintaining an extended effect in this model.

To understand the effects of aPC on CNS and immune cells, we separately isolated peritoneal macrophages, astrocytes and T cells and activated them *in vitro* with either lipopolysaccharide (LPS) or

Table 2 | Summary of the proteomic data

	AP	CAP	CP	CTL
Peptide	40,819	64,678	54,339	68,478
Unique peptide	6,321	10,143	8,967	8,991
Protein*	1,082	1,728	1,514	1,492
Reverse peptide identifications	39	34	10	12
Forward peptide identifications	3,612	4,937	3,687	4,020
False positive (%)†	1.08	0.69	0.27	0.3

* Identification filtering criteria: X_{corr} 1.9 (1+), 2.2 (2+), 3.7 (3+), delta correlation > 0.1, excluding trypsin, including keratin, excluding single peptide identification. The files used to compute false-positive rate were searched against concatenated forward and reverse human databases.
† Formula for the false positive (%): number of reverse identifications × 100/number of forward identifications, based on a representative subset of each category.

CD3/CD28 after pre-treatment with recombinant murine aPC. Activated macrophages and astrocytes treated with aPC produced less IL-6 and IL-17 (Fig. 5 d–g). Similarly, low levels of IL-17 were detected in T cells exposed to aPC (Fig. 5h). These data suggest that aPC suppresses inflammation in both the CNS and the periphery.

Because aPC suppressed NF-κB signalling during neuronal injury[27], we analysed protein extracts from cultured T cells treated with murine aPC in cell activation assays by western blot analysis. The results demonstrate less IκB breakdown in cells treated with aPC. This implies inhibition of NF-κB signalling by aPC (Fig. 5i).

Discussion

This study provides the first information on large-scale protein identification from highly characterized MS brain lesions. Proteomic expression profiling of MS brain lesions has identified several candidate therapeutic targets. Reversing the physiological effects of two of these newly implicated proteins (tissue factor and PCI) ameliorates disease in EAE. A parallel approach in identification of targets in EAE had previously led to development of new therapies in MS, as in the case of natalizumab, which targets a critical integrin involved in homing of monocytes to the inflamed brain[28]. Thus, this exercise has precedents in leading ultimately to new and effective therapies in MS.

Brück and Lucchinetti have classified active MS lesions according to their distinct histological and immunocytological characteristics[1]. The proteomic analysis of MS lesions illuminates the dynamic biological events that influence lesion development and pathogenesis. It will be possible to refine these proteomics techniques to analyse specific areas in MS tissues (for example, normal-appearing white matter, areas of oligodendrocyte destruction) in order to identify proteins unique to these particular regions of interest.

The reversal of neurological deficits in EAE by administration of thrombin inhibitor and aPC suggests several new options for MS therapy. Heparin therapy was shown to improve symptoms during MS relapses and active EAE[29,30], but treating patients with MS with an anticoagulant such as hirudin would not be optimal because of the increased risk of bleeding. Serum of EAE mice treated with hirudin also showed the presence of anti-hirudin antibodies (not shown), which may have interfered with the protective effects of hirudin during EAE. On the other hand, aPC may be a drug for future therapy in MS, especially if an aPC variant with reduced bleeding potential could be engineered by genetic modification[18,22].

Experiments using function-specific aPC mutants raise several intriguing questions about the pharmacological properties of aPC. Our results suggest that both the anticoagulant and signalling properties of aPC ameliorate EAE, perhaps through different mechanisms. One possible explanation consistent with our findings centres on PAR-1 activation such that either sending a cytoprotective signal

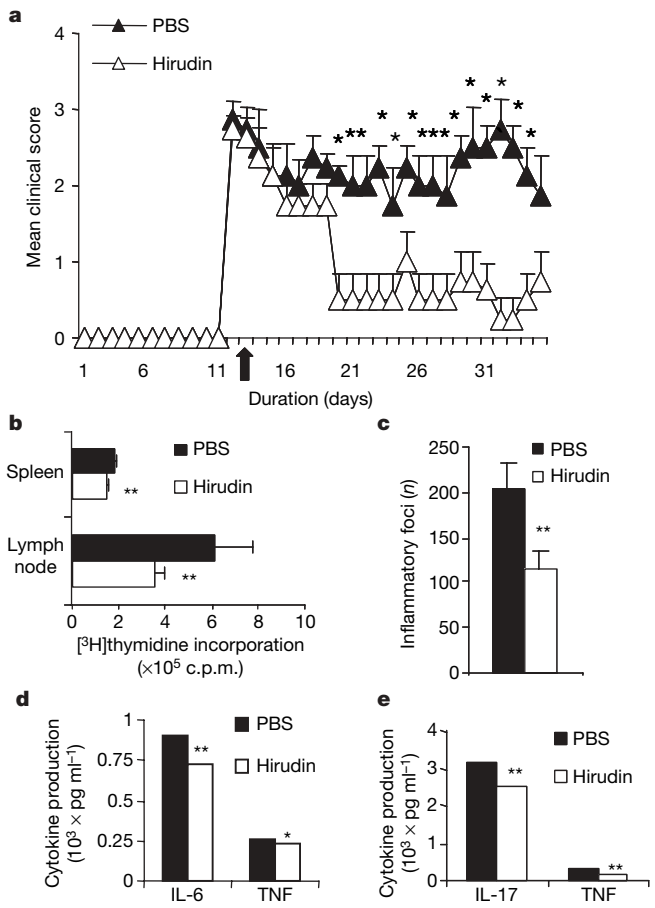

Figure 3 | Thrombin inhibition suppresses inflammation in EAE. **a**, Mean clinical scores ± s.e.m. of EAE mice treated with PBS (black) or recombinant hirudin (white) (10 mg kg^{-1}) ($n = 10$ per group) at the peak of disease (arrow) ($P < 0.05$, Mann–Whitney analysis). **b**, *In vitro* proliferation rates of splenocytes and lymph-node cells activated with PLP (20 μg ml^{-1}) and cytokine production from (**d**) splenocytes and (**e**) lymph-node cells of mice treated with PBS or hirudin. Mean ± s.e.m. *$P < 0.05$, **$P < 0.02$ (*t*-test) (from triplicate culture wells). **c**, Quantitation of inflammatory lesions from brain and spinal cord of EAE mice treated with PBS or hirudin ($n = 5$ per group). Data represent means ± s.e.m. (**$P < 0.01$).

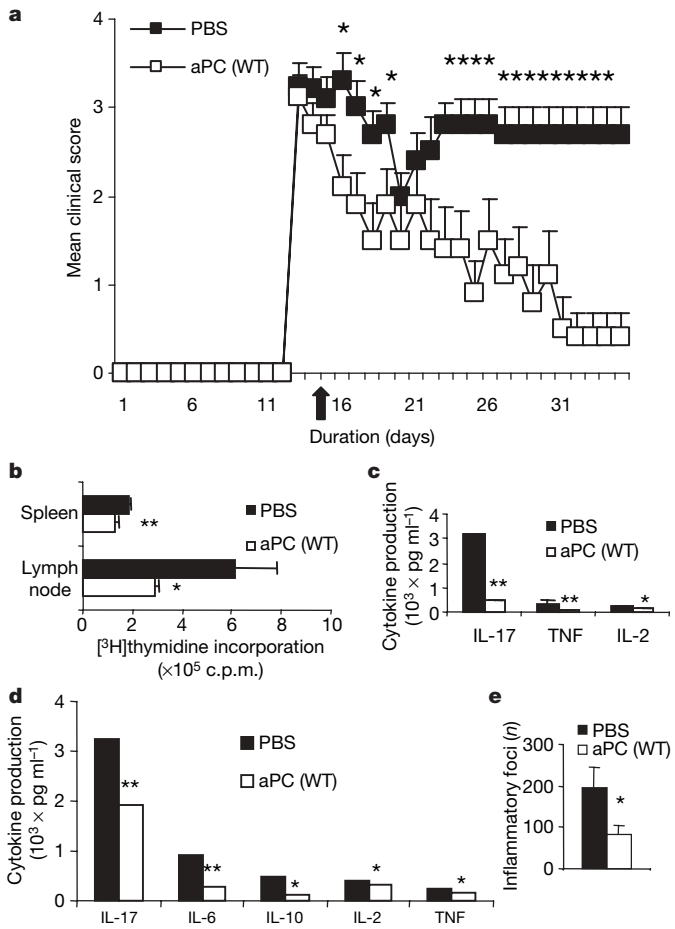

Figure 4 | aPC modulates Th1 and Th17 responses in EAE. **a**, Mean clinical scores ± s.e.m. of EAE mice treated with PBS (black) and aPC (white) at maximal paralysis (arrow) ($P < 0.05$, Mann–Whitney analysis); **b**, proliferation rates of splenocytes and lymph-node cells after activation with PLP peptide in culture and cytokine levels of c) lymph nodes and d) splenocytes from PBS and aPC-treated EAE mice. Means ± s.e.m. (picograms per millilitre) (*$P < 0.05$, **$P < 0.02$, *t*-test) **e**, Quantitation of inflammatory foci from paraffin-embedded sections from brain and spinal cord of EAE mice treated with PBS or aPC. Data represent mean ± s.e.m., ($P < 0.05$, *t*-test).

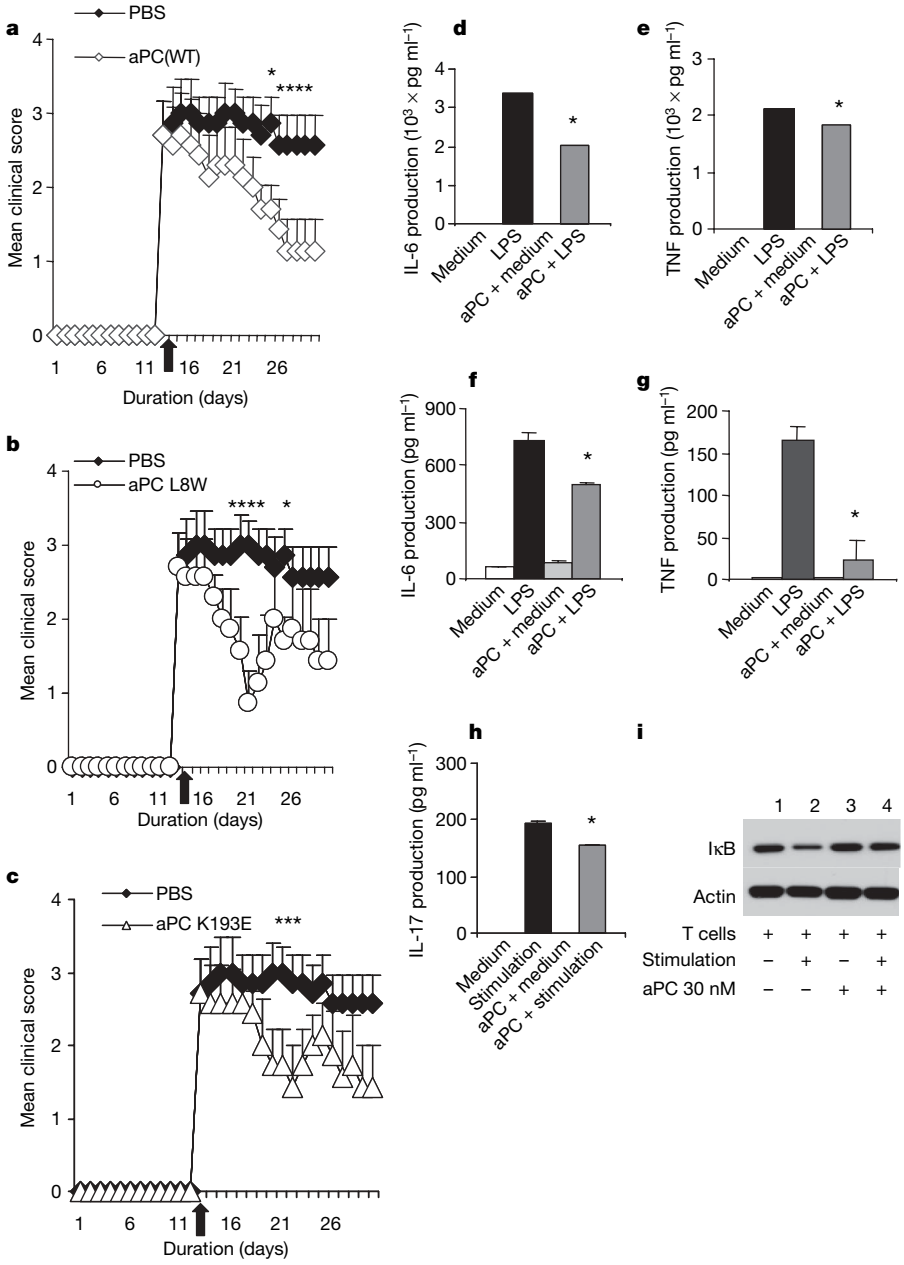

Figure 5 | Molecular mechanism of aPC during EAE. SJL/J mice with established EAE ($n = 7$ per group) were treated with (arrow) PBS or aPC-WT (**a**), aPC-L8W (**b**) or aPC-K193E (**c**) (0.46 mg kg^{-1}). Mean clinical scores ± s.e.m. (*$P < 0.05$, Mann–Whitney analysis). **d–h**, Macrophages (**d**, **e**), primary astrocytes (**f**, **g**) or purified T cells (**h**) were pre-treated with recombinant murine aPC-WT (30 nM) and activated with LPS (100 ng ml^{-1}) (**d–g**) or CD3/CD28 (5 μg ml^{-1}) (**h**), and cytokine levels were measured from culture supernatant. Means ± s.e.m. (pictograms per millilitre) ($P < 0.05$, *t*-test). **i**, Immunoblot of total cell lysate (50 μg) from purified T cells treated with aPC (30 min time point) probed with anti-IκB-α.

(through EPCR and PAR-1 by aPC-K193E) or inhibiting the generation of thrombin (by aPC-L8W, and thus suppressing its pro-inflammatory signals through PAR-1) is independently sufficient to improve function in EAE. Experiments to understand the molecular interplay of EPCR, PAR-1 and aPC signalling in the CNS and immune cells are underway. This may provide a direct application for MS therapy because PAR-1 signalling alone by aPC was sufficient to suppress EAE.

We used the approach of systems biology to identify the molecular composition of the proteins in defined MS lesions. The lesion-specific proteome reveals a 'new world', with most of the unique proteins identified in all three MS lesions possessing functions currently unknown within today's knowledge of physiology. Other proteins whose functions are known, like those of the coagulation cascade, are clearly playing new and perhaps unexpected pathobiological roles beyond our current understanding. The intersection of the coagulation cascade and inflammation in MS is the first of many new discoveries that will emerge from such a catalogue of proteins. These proteomes constitute a mere vocabulary for the biological language whose rules and structures must be deciphered to understand a disease like MS.

METHODS SUMMARY

Histopathological characterization of MS lesions. Cryosections from MS and control samples were analysed by H&E, LFB and immunohistochemistry as previously described[9]. MS lesions were classified according to the criteria used by Lock *et al.*[11]. Normal control brain samples were ruled out for obvious CNS pathology.

LCM, in-gel trypsin digestion, mass spectrometry, database searching. Cryosections (15 μM) from brain samples were cut on Molecular Machines and Industries (MMI) membranes and MS lesions were isolated by LCM as previously described[31]. Protein samples were extracted and resolved by

one-dimensional SDS–polyacrylamide gel electrophoresis (SDS–PAGE). Then, protein bands were digested with trypsin, and tryptic peptides were analysed repeatedly (four to seven times) with a linear trap quadrupole (LTQ) ion-trap mass spectrometer[13]. Data obtained from each gel band were searched independently against a non-redundant human protein database using the SEQUEST algorithm[32]. Files from acute plaque, CAP and chronic plaque were then combined using the INTERACT program[33] and filtered as previously described[12,34]. False-positive rates were estimated by searching against a concatenated forward and reverse human protein database[35].

EAE. EAE was induced in 7- to 8-week-old SJL/J female mice by subcutaneous immunization with 100 μg $PLP_{139–151}$ in emulsion[36]. For hirudin (Refludan, recombinant lepirudin, Berlex) or aPC treatment, EAE mice ($n = 10$ per group) were treated with daily intravenous injection of hirudin (10 mg kg^{-1}) or mouse recombinant aPC-WT (0.2 mg kg^{-1}) beginning at the peak of disease. Mice were assessed daily and scored according to: 0, no clinical disease; 1, tail weakness; 2, hindlimb weakness; 3, complete hindlimb paralysis; 4, hindlimb paralysis and some forelimb weakness; 5, moribund or dead.

Statistical analysis. Data are presented as means ± s.e.m. A *t*-test ($n = 2$ groups) was used for parametric data, and a Mann–Whitney *U*-test for non-parametric data ($n = 2$ groups) to detect between-group differences. A P value of 0.05 or lower was considered significant.

Full Methods and any associated references are available in the online version of the paper at www.nature.com/nature.

Received 25 October; accepted 20 December 2007.
Published online 17 February 2008.

1. Lassmann, H., Bruck, W. & Lucchinetti, C. Heterogeneity of multiple sclerosis pathogenesis: implications for diagnosis and therapy. *Trends Mol. Med.* **7,** 115–121 (2001).
2. Frohman, E. M., Racke, M. K. & Raine, C. S. Multiple sclerosis – the plaque and its pathogenesis. *N. Engl. J. Med.* **354,** 942–955 (2006).
3. Wekerle, H. Immune pathogenesis of multiple sclerosis. *Neurol. Sci.* **26** (suppl. 1), S1–S2 (2005).
4. Benito, C. *et al.* Cannabinoid CB1 and CB2 receptors and fatty acid amide hydrolase are specific markers of plaque cell subtypes in human multiple sclerosis. *J. Neurosci.* **27,** 2396–2402 (2007).
5. Kagitani-Shimono, K. *et al.* Lipocalin-type prostaglandin D synthase (beta-trace) is upregulated in the αB-crystallin-positive oligodendrocytes and astrocytes in the chronic multiple sclerosis. *Neuropathol. Appl. Neurobiol.* **32,** 64–73 (2006).
6. Minn, A. J. *et al.* Genes that mediate breast cancer metastasis to lung. *Nature* **436,** 518–524 (2005).
7. Rubinsztein, D. C. & Serra, H. G. Protein–protein interaction networks in the spinocerebellar ataxias. *Genome Biol.* **7,** 229.1–229.3 (2006).
8. Sam-Yellowe, T. Y. *et al.* A *Plasmodium* gene family encoding Maurer's cleft membrane proteins: structural properties and expression profiling. *Genome Research* **14,** 1052–1059 (2004).
9. Chabas, D. *et al.* The influence of the proinflammatory cytokine, osteopontin, on autoimmune demyelinating disease. *Science* **294,** 1731–1735 (2001).
10. John, G. R. *et al.* Multiple sclerosis: re-expression of a developmental pathway that restricts oligodendrocyte maturation. *Nature Med.* **8,** 1115–1121 (2002).
11. Lock, C. *et al.* Gene-microarray analysis of multiple sclerosis lesions yields new targets validated in autoimmune encephalomyelitis. *Nature Med.* **8,** 500–508 (2002).
12. Peng, J., Elias, J. E., Thoreen, C. C., Licklider, L. J. & Gygi, S. P. Evaluation of multidimensional chromatography coupled with tandem mass spectrometry (LC/LC-MS/MS) for large-scale protein analysis: the yeast proteome. *J. Proteome Res.* **2,** 43–50 (2003).
13. Hwang, S. I. *et al.* Systematic characterization of nuclear proteome during apoptosis: a quantitative proteomic study by differential extraction and stable isotope labeling. *Mol. Cell. Proteomics* **5,** 1131–1145 (2006).
14. Lundgren, D. H., Eng, J., Wright, M. E. & Han, D. K. PROTEOME-3D: an interactive bioinformatics tool for large-scale data exploration and knowledge discovery. *Mol. Cell. Proteomics* **2,** 1164–1176 (2003).
15. Esmon, C. T. Crosstalk between inflammation and thrombosis. *Maturitas* **47,** 305–314 (2004).
16. Eddleston, M. *et al.* Astrocytes are the primary source of tissue factor in the murine central nervous system. A role for astrocytes in cerebral hemostasis. *J. Clin. Invest.* **92,** 349–358 (1993).
17. Riewald, M. & Ruf, W. Orchestration of coagulation protease signaling by tissue factor. *Trends Cardiovasc. Med.* **12,** 149–154 (2002).
18. Mosnier, L. O., Zlokovic, B. V. & Griffin, J. H. The cytoprotective protein C pathway. *Blood* **109,** 3161–3172 (2007).
19. Song, X., Huhle, G., Wang, L., Hoffmann, U. & Harenberg, J. Generation of anti-hirudin antibodies in heparin-induced thrombocytopenic patients treated with r-hirudin. *Circulation* **100,** 1528–1532 (1999).
20. de Kleijin, E. D. *et al.* Activation of protein C following infusion of protein C concentrate in children with severe meningococcal sepsis and purpura fulminans: a randomized, double-blinded, placebo-controlled, dose-finding study. *Crit. Care Med.* **31,** 1839–1847 (2003).
21. Laterre, P. F. *et al.* Severe community-acquired pneumonia as a cause of severe sepsis: data from the PROWESS study. *Crit. Care Med.* **33,** 952–961 (2005).
22. Bernard, G. R. *et al.* Efficacy and safety of recombinant human activated protein C for severe sepsis. *N. Engl. J. Med.* **344,** 699–709 (2001).
23. Kirichuk, V. F. & Streknev, A. G. Rol' sistemy gemostaza v patogeneze i techenii rasseiannogo skleroza. *Zh. Nevrol. Psikhiatr. Im. S S Korsakova* (special issue 2), **103,** 34–38 (2003).
24. Gerlitz, B. G. Mutation of protease domain residues Lys37–39 in human protein C inhibits activation by the thrombomodulin-thrombin complex without affecting activation by free thrombin. *J. Biol. Chem.* **271,** 22285–22288 (1996).
25. Grinnell, B. W. *et al.* Differentiation of cytoprotective vs. anticoagulant function with variants of activated protein C in LPS-induced renal microvascular dysfunction. *Crit. Care Med.* **35,** (suppl.) abstr. 42 (2007).
26. Preston, R. J. *et al.* Multifunctional specificity of the protein C/activated protein C Gla domain. *J. Biol. Chem.* **281,** 28850–28857 (2006).
27. Cheng, T. *et al.* Activated protein C inhibits tissue plasminogen activator-induced brain haemorrhage. *Nature Med.* **12,** 1278–1285 (2006).
28. Steinman, L. Blocking adhesion molecules as therapy for multiple sclerosis: natalizumab. *Nature Rev. Drug Discov.* **4,** 510–518 (2005).
29. Maschmeyer, J., Shearer, R., Lonser, E. & Spindle, D. Heparin potassium in the treatment of chronic multiple sclerosis. *Bull. Los Angel. Neuro. Soc.* **26,** 165–171 (1961).
30. Lider, O. *et al.* Suppression of experimental autoimmune diseases and prolongation of allograft survival by treatment of animals with low doses of heparins. *J. Clin. Invest.* **83,** 752–756 (1989).
31. Bagnato, C. *et al.* Proteomics analysis of human coronary athrosclerosis plaque: a feasibility study of direct tissue proteomics by liquid chromatography and tandem mass spectrometry. *Mol. Cell. Proteomics* **6,** 1088–1102 (2007).
32. Yates, J. R. III, Eng, J. K., McCormack, A. L. & Schieltz, D. Method to correlate tandem mass spectra of modified peptides to amino acid sequences in the protein database. *Anal. Chem.* **67,** 1426–1436 (1995).
33. Han, D. K., Eng, J., Zhou, H. & Aebersold, R. Quantitative profiling of differentiation-induced microsomal proteins using isotope-coded affinity tags and mass spectrometry. *Nature Biotechnol.* **19,** 946–951 (2001).
34. Liu, H., Sadygov, R. G. & Yates, J. R. III. A model for random sampling and estimation of relative protein abundance in shotgun proteomics. *Anal. Chem.* **76,** 4193–4201 (2004).
35. Peng, J. *et al.* A proteomics approach to understanding protein ubiquitination. *Nature Biotechnol.* **21,** 921–926 (2003).
36. Platten, M. *et al.* Treatment of autoimmune neuroinflammation with a synthetic tryptophan metabolite. *Science* **310,** 850–855 (2005); erratum **311,** 954 (2006).

Supplementary Information is linked to the online version of the paper at www.nature.com/nature.

Acknowledgements We thank Mary Jane Eaton for help with histopathology and Jian Luo for help with imaging microscopy. This work was funded by the National Institutes of Health and the National Multiple Sclerosis Society to L.S., the National Institutes of Health to D.H., and Ruth L. Kirschstein National Research Service Award and T32 Adult and Pediatric Rheumatology and Immunology Fellowship awards to M.H.H. B.W.G. and B.G. are employed by Lilly Research Laboratories, a division of Eli Lilly & Co.

Author Contributions M.H.H. and L.S. formulated the hypothesis and designed all the experiments. D.K.H., S.-I.H. and D.H.L. contributed the proteomic studies. D.B.R. performed the EAE experiment with hirudin treatment. R.A.S. and C.S.R. contributed to the histopathological analysis. B.G. and B.W.G. provided the recombinant aPC proteins. J.V.P. performed studies on NF-κB signalling. S.S.O. performed the *in vitro* assays with astrocytes. D.K.H. and L.S., the senior authors, contributed equally to this work.

Author Information Reprints and permissions information is available at www.nature.com/reprints. The authors declare competing financial interests: details accompany the full-text HTML version of the paper at www.nature.com/nature. Correspondence and requests for materials should be addressed to L.S. (steinman@stanford.edu).

METHODS

Materials. All solvents, high-performance liquid chromatography (HPLC) or mass spectrometry grade, and reagents for histology were from Fisher. Metal-rim slides and micro-centrifuge tubes for LCM were from MMI. Recombinant murine aPC, recombinant human aPC-WT and mutants (aPC-L8W and aPC-K193E) were provided by Lilly Research Laboratories. Protease inhibitor cocktail tablets were from Roche Applied Science. ABC kit, secondary antibodies (biotinylated horseradish peroxidase conjugates) and diaminobenzidine were from Vector Inc. Monoclonal anti-GFAP (Glial fibrillary acidic protein), anti-CD3, anti-CD45 and anti-CD68 were from Dako Cytomation, and anti-CD28 was from BD Biosciences. Rabbit polyclonal antibodies against IκB-α and β-actin were from Cell Signalling and Sigma, respectively. Monoclonal anti-PLP was prepared as described previously[37].

Human brain samples from MS cases and normal controls. Fresh frozen MS and normal control brain samples were obtained at autopsy under a protocol approved by the Institutional Review Board. MS brain samples and accompanying paraffin-embedded sections were provided by C. S. Raine. Normal control samples were obtained from the University of Washington Alzheimer's Disease Brain Consortium. Samples were harvested, rapidly frozen and stored at –80 °C. All samples were obtained from the cerebral hemispheres.

Histopathological characterization and classification of MS lesions. Unfixed, frozen brain tissue from MS and control samples was partly thawed. Tissue blocks of about 1 cm were embedded in optimal cutting temperature compound (Sakura Finetek). Frozen blocks were cut into 6 μM cryosections, then fixed in acetone briefly and analysed by H&E, LFB and immunohistochemistry staining with antibodies against PLP, GFAP, CD3, CD45 and CD68 as previously described[9]. MS lesions were classified according to the criteria used by Lock *et al.*[11]. Normal control brain samples were ruled out for obvious CNS pathology.

Isolation of MS plaques by LCM and sample preparation. The LCM microscope and laser system were from MMI Systems. MS lesions were isolated from samples (frozen blocks) used for histological characterization. Sections (15 μM) were cut on MMI membranes, briefly fixed in 75% ethanol, and MS lesions were then isolated by LCM as previously described[31]. MS lesions from 400 tissue sections were isolated and extracted first with modified RIPA buffer (10 mM Tris-HCl, pH 7.5, 150 mM NaCl, 0.1% SDS, 1% Triton X-100, 1% deoxycholate, 5 mM EDTA, supplemented with protease inhibitor cocktail) and subsequently with 2% SDS buffer (62.5 mM Tris-HCl, pH 7.5, 2% SDS) for 15 min each at 65 °C. White matter from the control samples was also isolated in a similar manner.

In-gel trypsin digestion, nanoliquid chromatography and tandem mass spectrometry. Protein extracts (100 μg per sample) from MS and control brain samples were resolved by one-dimensional SDS–PAGE using a 4–12% NuPAGE gel (Invitrogen) and stained with Coomassie brilliant blue G-250. Protein bands (20 per sample) were then digested with trypsin and peptides extracted as described[13]. Tryptic peptides were analysed with an LTQ linear ion-trap mass spectrometer (Thermo Finnigan) equipped with a commercial nanospray source (Thermo Finnigan). Samples were loaded into an in-house C18 micro-column (100 μm inner diameter, 360 μm outer diameter, 10 cm length, 5 μm bead size, 100 Å pore size, Column Engineering Inc.) by a microautosampler (Famos-Dionex) and separated by an Agilent 1,100 high-performance binary pump. Peptides were loaded for 20 min with solvent A (5% acetonitrile, 0.4% acetic acid and 0.005% heptafluorobutyric acid) at a flow rate of about 200 nl min^{-1} by flow splitting. The solvent gradient of HPLC was linear from 95% solvent A to 30% solvent B (100% acetonitrile, 0.4% acetic acid and 0.005% heptafluorobutyric acid) for 45 min. The column was then regenerated by 80% solvent B for 10 min and 100% solvent A for 10 min. The eluent was introduced directly into an LTQ mass spectrometer by electrospray ionization. Each full mass-spectrometric scan was followed by a five tandem mass-spectrometry scan of the most intense ions with data-dependent selection using the dynamic exclusion option (top 5 method). Dynamic exclusion features were enabled to maximize the fragmentation of low-abundance peptide ions. Sample loading, solvent delivery and scan functions were obtained by XCalibur software (Thermo Finnigan). Each sample was analysed four to seven times by mass spectrometry.

Database searching and data processing. Data obtained from each gel band generated a .dat file and were searched independently against a non-redundant human protein database (56,709 entries as of 1 December 2004, Advanced Biomedical Computing Center) using the SEQUEST algorithm, resulting in one .html output file[32]. All .html files from each lesion type (acute plaque, CAP, chronic plaque) were combined using the INTERACT program[33]. They were then filtered with the following criteria: peptide mass tolerance of 2.0 with differential modification of +16 for oxidized methionine, +80 for phosphorylated serine, threonine and tyrosine, cross-correlation (Xcorr) of 1.9, 2.2 and 3.7 for 1+, 2+ and 3+ charge-state peptides, respectively, and delta correlation score greater than or equal to 0.1, excluding single peptide identification[12,34]. False-positive rates were estimated by searching a subset of acute plaque, CAP, chronic plaque and control samples against a concatenated forward and reverse human protein database using the following formula: false positive (%) = number of reverse peptide identifications × 100/number of forward peptide identification, based on representative subsets of each category[35] (Table 2).

Protein quantitation. Semi-quantitative protein abundance was estimated by spectral count. Spectral count was the number of tandem mass spectrometric spectra confidently assigned to the protein, as previously defined[34].

Identification of proteins unique to MS lesions and functional annotation. We used INTERSECT software to determine proteins unique to each lesion type[13]. Gene ontology (GO) classification and PROTEOME-3D software were then applied to assign biological functions and subcellular localization of these proteins[14].

EAE induction, treatment with hirudin, aPC (WT and mutants), proliferation assays, cytokine analysis and quantitative histopathology. Mice were maintained in the Research Animal Facility at Stanford University. EAE was induced in 7- to 8-week-old SJL/J female mice by subcutaneous immunization with 100 μg $PLP_{139–151}$ in emulsion[36]. For hirudin or aPC treatment, EAE mice ($n = 10$ per group) were treated with daily intravenous injection of hirudin (10 mg kg^{-1}) or mouse recombinant aPC-WT (0.2 mg kg^{-1}) at the peak of disease and compared with the PBS-treated group. Mice were assessed daily for clinical signs of EAE and scored according to: 0, no clinical disease; 1, tail weakness; 2, hindlimb weakness; 3, complete hindlimb paralysis; 4, hindlimb paralysis and some forelimb weakness; 5, moribund or dead.

Recombinant human aPC-WT and mutants (aPC-L8W and aPC-K193E) were prepared as described by Grinnell *et al.*[25]. These aPC variants have the following properties on aPTT and PAR-1 signalling function: aPC-WT: aPTT (relative activity) = 1, PAR-1 (relative activity) = 1; aPC-L8W: aPTT = 1, PAR-1 = 0.02; and aPC-K193E: aPTT = 0.03, PAR-1 = 1. EAE mice ($n = 7$/group) were treated with daily intravenous injection of recombinant human aPC-WT, aPC-L8W, aPC-K193E (0.46 mg kg^{-1}) or PBS (control group) at the time of maximal paralysis and assessed daily until day 30.

In vitro immune cell proliferation and cytokine analysis were performed as previously described[38]. Briefly, splenocytes and lymph-node cells harvested from EAE experiments were cultured in flat-bottomed, 96-well plates at a concentration of 0.5×10^6 cells per well in stimulation media (RPMI 1640 supplemented with 2 mM L-glutamine, 1 mM sodium pyruvate, 0.1 mM non-essential amino acids, 100 U ml^{-2} penicillin, 0.1 mg ml^{-2} streptomycin, 0.5 μM 2-mercaptoethanol and 10% FCS) and activated with $PLP_{139–151}$ peptide (5–20 μg ml^{-1}). To determine proliferation rates, cultures were pulsed with [^{3}H]thymidine (1 μCi per well) after culture for 72 h and harvested 18 h later onto filter paper. The c.p.m. of incorporated [^{3}H]thymidine was read with a beta counter. Cytokine levels (IL-2, IL-4, IL-6, IL-10, IL-12p40, IL-17, IFN-γ, TNF) were measured from the supernatant of cultured cells using anti-mouse OptEIA ELISA kits (BD Pharmigen).

For histopathological analysis, brains and spinal cord of EAE mice were fixed in 10% formaldehyde. Paraffin sections (6 μM thick) were stained with LFB and H&E. The number of inflammatory foci within the brain and spinal cord were quantified by a neuropathologist who was blinded to the treatment and clinical parameters of the mice.

***In vitro* immune cell activation assays and cytokine analysis.** T lymphocytes were isolated from pooled splenocytes and lymph node cells from 8-week-old naive SJL/J mice by negative selection (Pan T-cell isolation kit, Miltenyi Biotech). Cells were pretreated with 30 nM recombinant murine aPC for 15 min at 37 °C followed by activation with CD3/CD28 (5 μg ml^{-1}) coated on 12-well plates. Cells were cultured at 5×10^6 cells per millilitre concentration in stimulation media. Culture plates were harvested at different time points (15 min to 96 h) and cytokine levels were measured from culture supernatant by enzyme-linked immunosorbent assay (ELISA).

Primary peritoneal macrophages were isolated from naive 8- to 9-week-old SJL/J mice after intraperitoneal injection of thioglycollate (BD Diagnostic Systems) and cultured in complete medium (DMEM supplemented with 10% fetal bovine serum, 1 mM sodium pyruvate, 100 μM penicillin and 0.1 mg ml^{-1} streptomycin)[38]. Cells (1×10^6cells per millilitre) were treated with 30 nM recombinant murine aPC for 15 min, then activated with LPS 100 ng ml^{-1} (Sigma) and harvested at different time points (15 min to 72 h). Cytokine levels were then measured.

Astrocyte culture. Astrocytes were cultured from brain of one-day-old SJL/J pups as described previously[38]. Briefly, the cerebral cortices from pups were minced, cells were disrupted by passing through a filter and cultured in complete DMEM. Purified astrocytes (50–80% confluent) were treated with 30 nM recombinant murine aPC for 15 min and activated with 100 ng ml^{-1} LPS (Sigma). Cells

were harvested at 4, 24, 48 and 72 h, and supernatant analysed by ELISA for cytokine production.

Western blot analysis. For NF-κB activation, total cell lysates from purified T cells treated with aPC were analysed by SDS–PAGE, transferred to polyvinylidene fluoride membrane, probed with antibodies against IκB-α and β-actin, and the signal visualized by enhanced chemiluminescence[38].

Statistical analysis. Data are presented as means ± s.e.m. When data were parametric, a *t*-test ($n = 2$ groups) was used to detect between-group differences. When data were non-parametric, a Mann–Whitney *U*-test was used for comparison between groups ($n = 2$ groups). A P value of 0.05 or lower was considered significant. Error bars in Figs 3d, e, 4c, d and 5 d, e are not discernible because of their small size.

37. Greenfield, E. A. *et al.* Monoclonal antibodies to distinct regions of human myelin proteolipid protein simultaneously recognize central nervous system myelin and neurons of many vertebrate species. *J. Neurosci. Res.* **83,** 415–431 (2006).
38. Ousman, S. S. *et al.* Protective and therapeutic role for αB-crystallin in autoimmune demyelination. *Nature* **448,** 474–479 (2007).